



UvA-DARE (Digital Academic Repository)

Unusual increase in the 325 MHz flux density of PSR B0655+64

Galama, T.J.; de Bruyn, A.G.; van Paradijs, J.A.; Hanlon, L.; Bennet, K.

Publication date

1997

Published in

Astronomy & Astrophysics

[Link to publication](#)

Citation for published version (APA):

Galama, T. J., de Bruyn, A. G., van Paradijs, J. A., Hanlon, L., & Bennet, K. (1997). Unusual increase in the 325 MHz flux density of PSR B0655+64. *Astronomy & Astrophysics*, 325, 631-639.

General rights

It is not permitted to download or to forward/distribute the text or part of it without the consent of the author(s) and/or copyright holder(s), other than for strictly personal, individual use, unless the work is under an open content license (like Creative Commons).

Disclaimer/Complaints regulations

If you believe that digital publication of certain material infringes any of your rights or (privacy) interests, please let the Library know, stating your reasons. In case of a legitimate complaint, the Library will make the material inaccessible and/or remove it from the website. Please Ask the Library: <https://uba.uva.nl/en/contact>, or a letter to: Library of the University of Amsterdam, Secretariat, Singel 425, 1012 WP Amsterdam, The Netherlands. You will be contacted as soon as possible.

Unusual increase in the 325 MHz flux density of PSR B0655+64

T.J. Galama¹, A.G. de Bruyn^{2,3}, J. van Paradijs^{1,4}, L. Hanlon⁵, and K. Bennett⁶

¹ Astronomical Institute ‘Anton Pannekoek’/CHEAF, Kruislaan 403, 1098 SJ, Amsterdam, The Netherlands

² NFRA, Radio Observatory, Postbus 2, 7990 AA, Dwingeloo, The Netherlands

³ Kapteyn Astronomical Institute, Postbus 800, 9700 AV, Groningen, The Netherlands

⁴ Physics Department, UAH, Huntsville, AL 35899, USA

⁵ Physics Department, University College Dublin, Belfield, Dublin 4, Ireland

⁶ Astrophysics Division, ESTEC, Noordwijk, The Netherlands

Received 19 July 1996 / Accepted 12 November 1996

Abstract. We report on the detection of a large amplification of the flux density of PSR B0655+64 at 325 MHz (a factor of ~ 43) that lasted about one hour. To the best of our knowledge such a large amplification has not been reported before. The phenomenon is restricted to a very narrow bandwidth (50 % decorrelation half-width of 3.6 ± 0.4 MHz). The decorrelation bandwidth and characteristic time scale of the variation are in agreement with the values expected for diffractive interstellar scintillation. However, the observed amplification of the flux density of PSR B0655+64 is rather large. The observations suggest that amplifications of a factor up to 8 are not uncommon for PSR 0655+64 at 92 cm. The extreme flux density amplification of PSR 0655+64 might be explained in terms of caustics. We consider it unlikely that this event can be explained by intrinsic variability.

Key words: pulsars: individual: PSR B0655+64 – scattering – radio continuum: ISM

1. Introduction

Pulsar intensity variations may be divided roughly into three classes. Rapid pulse to pulse variations, on time scales of milliseconds to minutes, are intrinsic to the pulsar emission mechanism; these pulse to pulse variations can be very strong (e.g., Cognard et al. 1996). On longer time scales, pulsars reveal variations of minutes to hours, and variations with time scales of days to months. The long-term variations are believed to be extrinsic to the pulsars; the source of these variations has been identified with irregular plasma refraction by the interstellar medium between the source and the observer (interstellar scintillation, ISS; see for reviews of the subject Narayan 1992; Rickett 1977, 1990). Rickett et al. (1984) pointed out that ISS occurs on two

time scales. The variations on time scales of minutes to hours are caused by the familiar diffractive interstellar scintillation (DISS e.g., Scheuer 1968; Salpeter 1969; Manchester & Taylor 1977). This scintillation causes a modulation of the pulsar flux density in time and frequency. It has only recently been established that the variations on time scales of days to months are produced by refractive interstellar scintillation (RISS).

The reported refractive modulation indices m_{ref} were substantially greater than predicted by a simple Kolmogorov spectrum model ($\beta=11/3$, Rickett & Lyne 1990). Modifications of the pure Kolmogorov spectrum have been proposed in attempts to explain the enhanced levels of refractive scintillation. The steep spectrum model ($\beta > 4$, Blandford & Narayan 1985; Goodman & Narayan 1985) and the inner scale model (Coles et al. 1987) predict enhanced levels of refractive interstellar scintillation. Strongly non-Gaussian “spikes” have been reported in long-term pulsar flux monitoring (e.g., Cole et al. 1970; Helfand et al. 1977). Goodman et al. (1987) argued that these might be due to strong focussing events or caustics. They suggest that caustics can arise when the power law spectrum of the electron density inhomogeneities is truncated at an inner or cut-off scale r_c , intermediate between the diffractive scale r_{dif} and the refractive scale r_{ref} . Caustics then contribute to the interstellar scintillation on an intermediate scale, r_{int} ; intermediate between the cut-off, r_c , and refractive, r_{ref} , scale. Particularly striking events, due to strong refractive focussing, so called Fiedler events, have been observed in radio quasars (Fiedler et al. 1987). In the most dramatic event Fiedler et al. observed intensity increases of roughly threefold on refractive time scales (80–100 days). Romani et al. (1987) explained this event in terms of caustics resulting from refraction by a large structure.

In this paper we present the discovery of a very large amplification of the flux density of PSR B0655+64 at 325 MHz. We discuss our observing and analysis procedures in Sect. 3 and present the results of the observations in Sect. 4. We discuss our findings in Sect. 5 and summarize our conclusions in Sect. 6.

2. PSR B0655+64

PSR B0655+64 was discovered in the pulsar survey by Damashek et al. (1978). It was recognized as a member of a binary system in 1982 (Damashek et al. 1982). It has a pulse period of 0.196 s and orbital period of 24.7 h (Lyne 1984). The pulsar has a very small period derivative of $6.9 \times 10^{-19} \text{ s s}^{-1}$, which implies a spin-down age of $4.5 \times 10^9 \text{ yr}$, and a magnetic field strength of $1.2 \times 10^{10} \text{ G}$ (Jones & Lyne 1988). Its companion was identified to be a cool white dwarf (Kulkarni 1986). The pulsar has a dispersion measure of 8.74 pc cm^{-3} , indicating a rather small distance of about 300 pc (Lyne 1984). A spectral index $\alpha_s = -2.1 \pm 0.2$ and flux densities of 5.2 ± 1.1 , 2.1 ± 0.5 , 2.3 ± 1.0 and $0.3 \pm 0.1 \text{ mJy}$ at 408, 606, 925 and 1408 MHz, respectively, have been given by Lorimer et al. (1995). These flux density measurements were made over a period of three to four years and provide a reliable estimate of the time averaged flux density. (Previously published data from pulsar surveys are likely to be subject to some uncertainty in their low-frequency flux densities, due to the long-term variations caused by refractive interstellar scintillation). The position of PSR B0655+64 from the catalog of Taylor et al. (1993) is $06^{\text{h}}55^{\text{m}}49.449^{\text{s}} \pm .06^{\text{s}}$, $+64^{\circ}22'23.157'' \pm .008''$ (B1950).

3. Observations and data reduction

In a program to search for the radio counterpart to gamma-ray bursts (GRBs), with the Westerbork Synthesis Radio Telescope (WSRT), the COMPTEL maximum-likelihood position of the strong GRB 940301, was observed frequently, over a time span of about six months at 21 and 92 cm. The 92 cm broad-band data cover a total bandwidth of 40 MHz, recorded in 8 bands each 5 MHz wide, centered at 319.3, 325, 333, 341, 355, 360, 375 and 380 MHz. A total of 48.8 hours of data were taken in 9 broad-band observations, covering a period from April 2 until June 25, 1994; additional observations were obtained January 15 and 16, 1996 (see Table 1 for details on the individual observations). All four polarisations are measured, but the cross hand signals only for the standard 40 (fixed-movable) interferometers. Due to interference about 20 % of the data were unusable. The data were reduced using the Netherlands East-West Synthesis Telescope Array Reduction package (NEWSTAR)¹.

Because of incompleteness of the $u - v$ coverage of observations that last less than 12 hours, we combined data from the April 2 observation with data from the June 25 observation, which, together, yielded an almost complete 12^{h} synthesis. From these data we constructed an accurate model of the field. After calibrating the complex gains, for each observation and each band, using the calibrator source 3C147 (for which we adopted a flux density of 56.7 Jy and a spectral index $\alpha_s = -0.62$ at 325 MHz), the data were self calibrated in gain and phase using a model of the field obtained from the initial data. This process was iterated a few times and thereby the model refined until all background sources above a flux density of about 6 mJy were

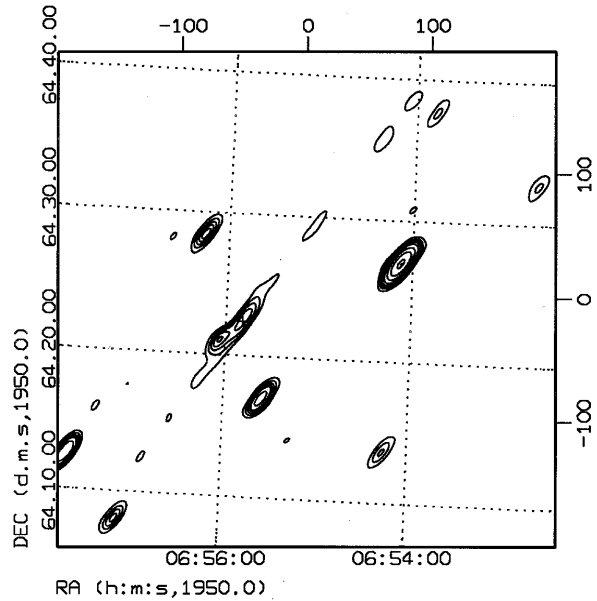


Fig. 1. Contour plot of a WSRT image at 325 MHz. The position of PSR B0655+64 is indicated by the cross. The plot shows the elongated structure of PSR B0655+64 in the image of June 25. Contour levels are 15, 30, 45, 60, 75, 120, 240, 480, 960 and 1075 mJy. Map noise is 3.6 mJy (1σ).

Table 1. Broad-band observations.

Day	Duration (h:m:s)	MJD ^a (start)
Apr. 2, 1994	5:15:46	49444.53712
Apr. 11, 1994	3:10:21	49453.77425
May 2, 1994	2:08:10	49474.73889
May 20, 1994	2:20:12	49492.75757
June 5, 1994	4:44:36	49508.61398
June 11, 1994	4:53:28	49514.46261
June 13, 1994	3:54:28	49516.32247
June 20, 1994	5:04:39	49523.55892
June 25, 1994	6:15:00	49528.49390
Jan. 15, 1996	6:08:50	50097.94238
Jan. 16, 1996	4:59:39	50098.78943

^a MJD = JD - 2400000.5

included in the model. Because of the relatively large baseline in frequency in the broad-band 92 cm data we also solved for the spectral index (where spectral index α_s is defined by $\alpha_s = d \log S / d \log \nu$) for each source in the field. Hereafter the spectral-index model (SI-model) was used for self calibration of all the data.

4. Results

4.1. Elongated structure

In the map obtained from data of June 25, 1994, we noticed a faint straight elongated structure, repeating itself at the grating

¹ <http://www.nfra.nl:80/newstar/>

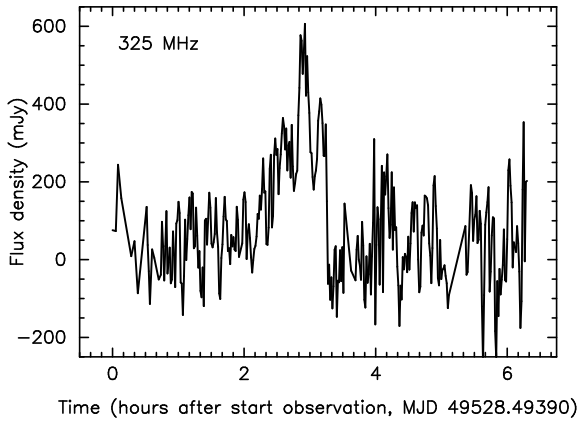


Fig. 2. Light curve at the position of PSR B0655+64 from the 92 cm observations of June 25, at 325 MHz. Integration time is 1 min. R.m.s. noise is 100 mJy (1σ).

response distances (see Fig. 1). The shape of the artifact is very similar to imperfections in the image caused by rapid refractive index changes of the ionosphere. Upon closer inspection we noticed that the particular feature was not associated with any of the brighter sources in the field. This excludes an explanation as an ionospheric effect. Moreover, the feature was detected at all interferometers. The elongated image response suggests that an object flared for only a short period of time (the instantaneous beam is a fan beam rotating clockwise). Such features have been observed from radio flares of nearby binary stars (e.g., Van den Oord & De Bruyn 1994). The Palomar sky survey did not reveal an optical counterpart down to its limiting magnitude (O and $E \sim 20 m$). This means that we can exclude the possibility that this flare was produced by a nearby (ordinary) binary star system. Moreover, we noticed that the phenomenon is quite restricted to the 325 MHz band. The flux density amplification is not observed in the adjacent frequency bands (see Fig. 3). The observation of a decorrelation bandwidth suggests that we are dealing with interstellar scintillation. Therefore we searched for a nearby pulsar in the catalog of Taylor et al. (1993) and found that, in fact, the feature and the binary pulsar PSR B0655+64 coincide to within $1.3''$ (correction for the proper motion of PSR B0655+64 is unimportant), in the direction perpendicular to the elongation. This confirmed that we observed interstellar scintillation.

4.2. Light curves

The change in intensity of PSR B0655+64 in the data of June 25, 1994, as a function of time was determined by construction of light curves (1 minute integration), as follows. We extracted the visibilities on the short baselines (< 1200 m., since long baselines suffer from bandwidth smearing, see Sect. 4.3), after subtracting the model (PSR B0655+64 was excluded from the model). We excluded the very short baselines (< 350 m.) and the interferometers that suffer from interference of the Westerbork observatory building. We then phase rotated the visibilities to

the position of PSR B0655+64, using the accurate position from the catalog of Taylor et al. (1993). Subsequently the visibilities were vector averaged. The real part (the cosine) of this averaged visibility corresponds to the amplitude of the signal from PSR B0655+64. We determine the r.m.s. noise in the light curves from the complex part (the sine). To obtain the amplitude we first had to correct for primary beam attenuation (factors 1.82, 1.86, 1.92, 1.99, 2.11, 2.16, 2.31 and 2.36 at 319.3, 325, 333, 341, 355, 360, 374.8 and 379.8 MHz, respectively; henceforth all quoted flux densities have been corrected for primary beam attenuation) and take into account the suppression caused by self calibration. Self calibration suppresses the observed brightness distribution not contained in the model used for the self calibration (e.g., Wieringa 1992). Since we excluded PSR B0655+64 from the model, used for self calibration, we have to make a correction for the reduction of its flux density. The reduction factor was determined by injecting about 10 artificial sources at “empty” places in the field and performing a new self calibration. We made two maps deconvolved with the model of the field, one with the “old” self calibration and one with the “new” self calibration, and obtained the difference map. The artificial sources appear in the difference map with the suppressed fraction of their flux density. The reduction factor was found to be 1.20 ± 0.03 .

The raw light curve (not smoothed, i.e., integration time of 1 min.) at 325 MHz, June 25, is shown in Fig. 2. The r.m.s. noise is 100 mJy (1σ ; henceforth all quoted errors are 1σ). There is no evidence in the light curves for large variations on a timescale of 1 minute. Therefore we smoothed the light curves with a triangular function of width 14 minutes, in order to obtain higher signal to noise. Those smoothed light curves at 319.3, 325, 333 and 341 MHz, respectively, are shown in Fig. 3.

The flare in the 325 MHz light curve (Figs. 2 and 3) reached its maximum at MJD 49528.614 (2.9 h after the start of the observation). In the non-smoothed light curve (Fig. 2) it has a peak of about 580 mJy (5.8σ); its duration is about one hour. Using an extrapolation of the flux densities given by Lorimer et al. (1995) we expect a flux density of $S_{325\text{MHz}} = 8.4 \pm 2.2$ mJy. This is consistent with the flux density (8 ± 1 mJy) measured in a 10^h observation of the same field on Jan. 15 and 16, 1996. This yields an amplification of a factor 69 ± 23 . The flare is more significant (7.3σ) in the smoothed light curve (Fig. 3). Due to the smoothing, the peak has decreased to about 400 mJy.

4.3. Decorrelation bandwidth

The light curves in adjacent frequency bands (Fig. 3) do not reveal a significant increase in the flux density, at the time of the flux increase at 325 MHz. Clearly the phenomenon is restricted to a very narrow bandwidth. Due to the finite width of the observing band (5 MHz) the peak amplitude sets a lower limit to the amplification. However, we have good evidence that the spectral width of the ‘flare’ is in fact a significant fraction of the 5 MHz because we see the full effect of bandwidth smearing in the visibilities as a function of baseline. At the time of the flare the fanbeam of the array was oriented almost orthogonal to the

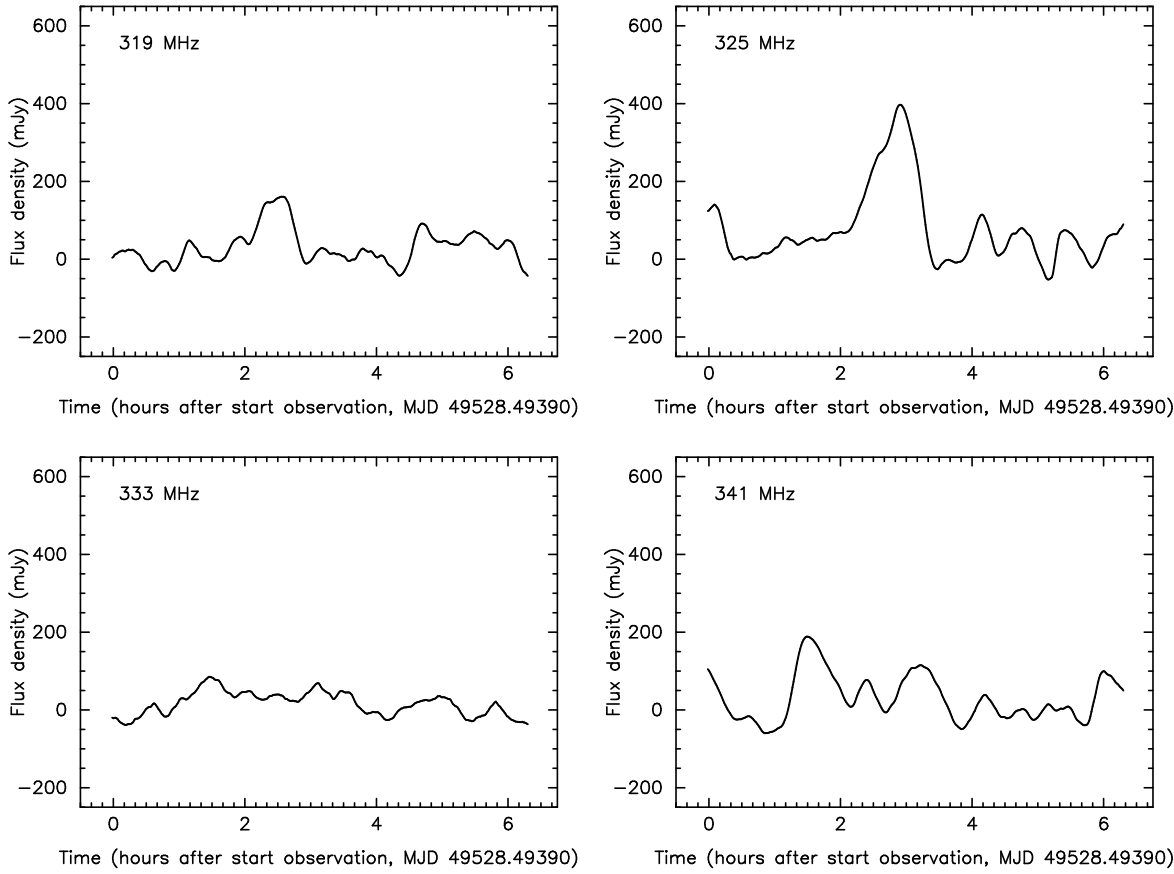


Fig. 3. Light curves at the position of PSR B0655+64 from the 92 cm observations of June 25. Smoothed with a triangular function of width 14 min. From upper-left to down-right corner 319.3, 325, 333, and 341 MHz. R.m.s. noises are 40, 55, 35 and 50 mJy (1σ), respectively.

direction to the phase-centre implying that the effects of bandwidth smearing were close to their maximal value. Assuming that the phenomenon has a Gaussian profile $H(\nu)$ as a function of frequency ν

$$H(\nu) = \sqrt{\frac{\ln 2}{\pi}} \frac{1}{\Delta\nu} \exp \left[-\ln 2 \left(\frac{\nu}{\Delta\nu} \right)^2 \right], \quad (1)$$

we can derive the 50% decorrelation half width, or decorrelation bandwidth $\Delta\nu$ as follows.

For an East-West interferometer the visibility function V takes the form

$$V = \int \int B(l, m) e^{-2\pi i \tau_g} dl dm, \quad (2)$$

$$\tau_g = -\frac{D}{c} (l \cos h_0 + m \sin \delta_0 \sin h_0) \nu, \quad (3)$$

where $B(l, m)$ is the sky-brightness distribution at position (l, m) (in radians, measured with respect to the phase tracking centre), τ_g is the geometrical delay, D is the baseline length, c is the speed of light, and h_0 and δ_0 are the hour angle and declination, respectively, of the phase-tracking centre. The smearing due to the Gaussian shape $H(\nu)$ results in a 'smeared' visibility V_{sm} , given by

$$V_{\text{sm}} = \int_0^\infty V H(\nu) d\nu = V \exp(\Phi_V), \quad (4)$$

$$\Phi_V = -\frac{1}{\ln 2} \left[\frac{\pi D}{c} (l \cos h_0 + m \sin \delta_0 \sin h_0) \Delta\nu \right]^2. \quad (5)$$

We determined the peak flux of the flare as a function of baseline D in 325 MHz light curves. The light curves were smoothed with a triangular function of width 14 min. and averaged over a range of baselines (348-996, 1008-1500, 1572-1932, 2004-2292 and 2508-2724 m.). The result is plotted in Fig. 4. A Gaussian fit revealed a baseline length $D_{1/2}$, at which the peak has decreased to 50%, of $D_{1/2} = 1.62^{+0.20}_{-0.15} 10^3$ m. Using Eqs. 4 and 5 we then find $\Delta\nu = 3.6 \pm 0.4$ MHz.

4.4. DISS behavior

In order to be sensitive to (probably) weaker events on other days (showing DISS) we averaged the data over a longer period. For all the 92 cm data we obtained flux densities of PSR 0655+64, using maps, made with 45 minutes of data. The 45 minutes have been chosen since it is the typical time scale for DISS of PSR B0655+64 at this frequency (see Sect. 5.1). For a study of DISS,

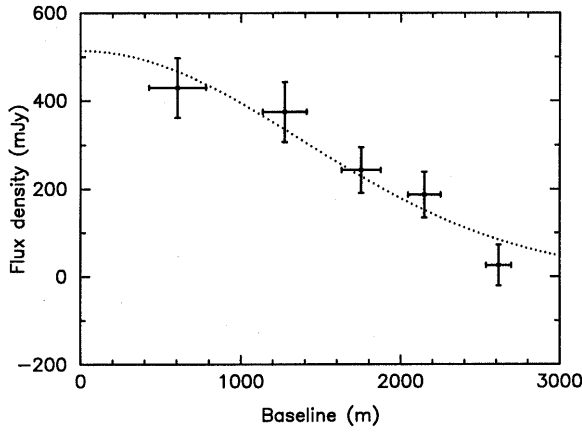


Fig. 4. 325 MHz flux density of the peak of the flare as a function of baseline. The peak values have been determined from light curves which have been smoothed with a triangular function of width 14 min. and have been averaged over a range of baselines. Also the Gaussian fit is shown.

smaller integration times would have been preferable, but then error bars would have become too large. In the following we will use the term “light curves” for results obtained by phase rotation, as distinct from the flux densities derived from maps.

Fig. 5 shows those flux densities as a function of time for all eight frequency bands (the errors are map noises). Note that in these plots, due to the relatively short integration time (45 min.) and the relatively small bandwidth (5 MHz) we are sensitive to DISS effects in both time and frequency.

As can be seen from Fig. 5, there is quite some scatter in the flux density, but the quiescent level of PSR B0655+64 is in agreement with 8.4 mJy in the better-quality bands (325, 341, 355 and 360 MHz).

For a quantitative measure of the departure from the average flux level of the data points in Fig. 5 we use the weighted average of the variance in the distribution of the intensity $\langle \Delta I \rangle_{\text{dis}}$. We have

$$\langle \Delta I \rangle_{\text{dis}} = \sqrt{\frac{\sum_i \frac{1}{\sigma_i^2} (I_i - \langle I \rangle)^2}{\sum_i \frac{1}{\sigma_i^2}}} \frac{N}{N-1}, \quad (6)$$

where σ_i is the map noise of the i th data point, and $\langle I \rangle$ the weighted average

$$\langle I \rangle = \frac{\sum_i \frac{1}{\sigma_i^2} I_i}{\sum_i \frac{1}{\sigma_i^2}}. \quad (7)$$

The average weighted variances $\langle \Delta I \rangle_{\text{dis}}$ are 31, 24, 24, 18, 16, 19, 25, and 17 mJy at 319, 325, 333, 341, 355, 360, 375 and 380 MHz, respectively.

It is clear that at 325 MHz the observation of June 25 (day 84) reveals a very significant flux density increase (152 ± 15 mJy, 6.3 times the scatter $\langle \Delta I \rangle_{\text{dis}}$). Due to the integration time of 45 minutes, band-width smearing and the shift of the

Table 2. Long-term flux density averages of PSR B0655+64.

Frequency (MHz)	\bar{I} (mJy)	$\bar{I}_{25\text{June}}$ (mJy)	\bar{I}_{event} (mJy)
319.3	3 ± 6	25 ± 11	49 ± 9
325	13.5 ± 2.1	18 ± 7	76 ± 7
333	15 ± 3	22 ± 8	28 ± 6
341	11.5 ± 1.9	19 ± 6	40 ± 7
355	12.1 ± 2.2	22 ± 7	28 ± 6
360	9.0 ± 2.9	12 ± 5	32 ± 6
375	19 ± 4	7 ± 7	16 ± 7
380	12.7 ± 8	28 ± 9	21 ± 10

event with respect to the 45 min. interval, the flux density is substantially lower than the 580 mJy peak (another high point is next to it).

Another increase in flux density is observed on June 13 (day 72). It is visible at 341 MHz (78 mJy, 4 times the scatter $\langle \Delta I \rangle_{\text{dis}}$) and at 355 MHz (82 mJy, 5.1 times the scatter $\langle \Delta I \rangle_{\text{dis}}$). The 78 mJy corresponds to an amplification by a factor of 10 ± 3 , extrapolating Lorimer et al.’s flux density values. Again, due to the previously mentioned reasons the peak values are likely to be stronger.

The 400 MHz flux density of 40 mJy from the discovery observations of Damashek et al. (1978; about eight times the long-term average given by Lorimer et al. 1995) and the June 13 increase, suggest that amplifications of a factor up to 8 are not extremely uncommon for PSR 0655+64 at low frequencies.

4.5. Average flux densities and RISS behavior

We have determined long-term average flux densities \bar{I} for PSR B0655+64 from our own data. We combined all the data from April to June, 1994, and excluded the observation in which we find the enhanced flux density (June 25, day ~ 84 in Fig. 5) in deriving the averages, \bar{I} (31.5 hrs of data).

The best estimates of the refractive “state” of the ISS on June 25 comes from “long-term” flux density averages. Unfortunately the duration of the June 25 observation is only 6.3 hrs (just about eight times the characteristic diffractive time scale of PSR B0655+64). We determined the average flux densities, $\bar{I}_{25\text{June}}$, over the June 25 observation (excluding the interval in which the event took place; from 1.3 to 4 hrs after the start of the observation; see Fig 2 and 3; total integration 3.6 hrs). And we determined the average flux densities \bar{I}_{event} (averages over the interval from 1.3 to 4 hrs after the start of the observation; total integration 2.7 hrs; the errors are map noises). The results are shown in Table 2.

Using our own long-term average flux density at 325 MHz for PSR B0655+64 (see Table 2), we find that the peak of the flare corresponds to an amplification of a factor 43 ± 9 .

We see from Table 2 that in most frequency bands the average flux densities for PSR B0655+64 are slightly higher on June 25 ($\bar{I}_{25\text{June}}$) and clearly higher during the event (\bar{I}_{event}).

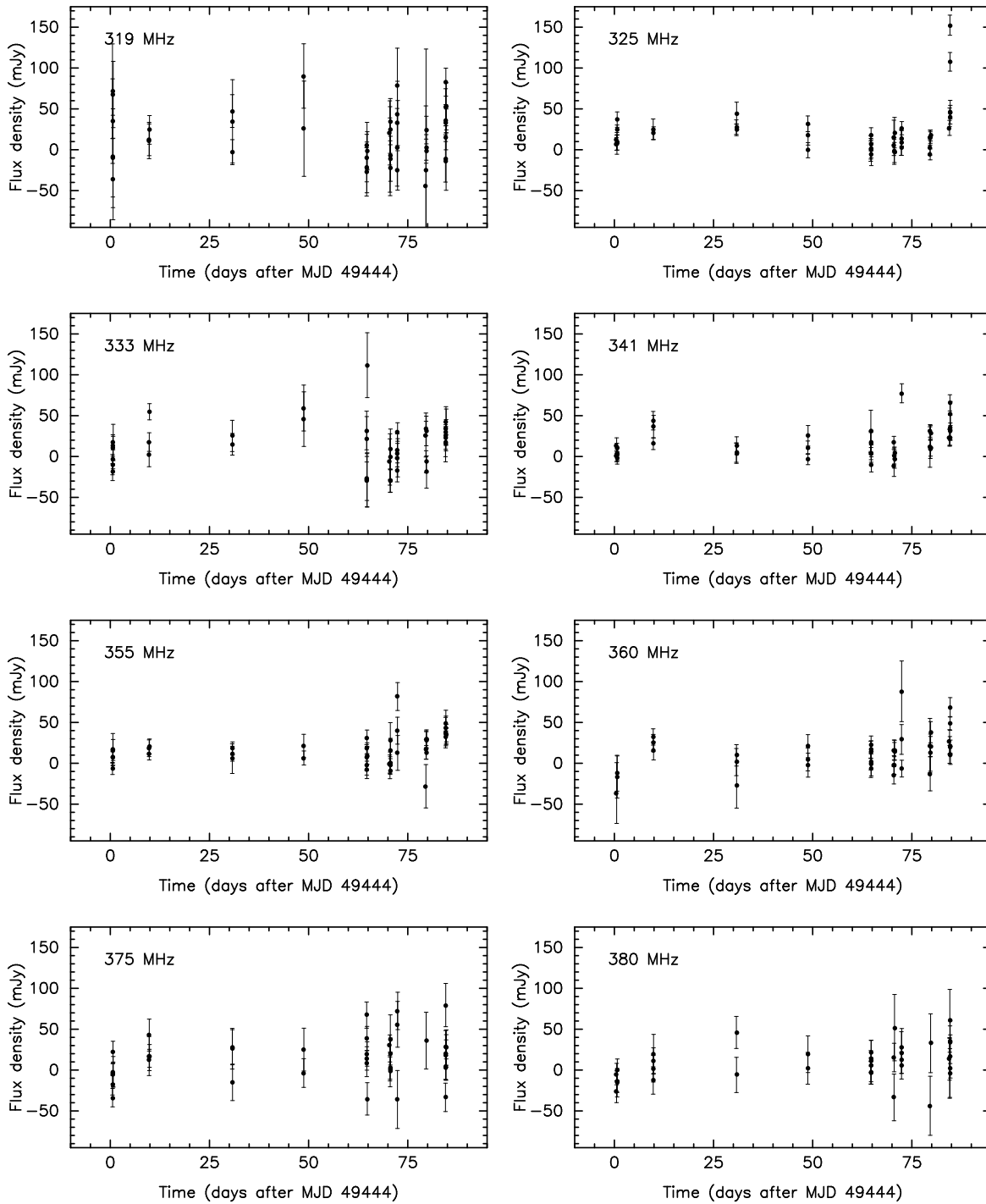


Fig. 5. Flux densities against time, in days after MJD 49444, at the position of PSR B0655+64 for all eight bands of the 92 cm observations. Averaging time is 45 minutes (typical time scale of the interstellar scintillation). From upper-left to down-right corner 319, 325, 333, 341, 355, 360, 375 and 380 MHz. The errors (1σ) are noises determined from the maps. The average weighted variances, $\langle \Delta I \rangle_{\text{dis}}$, are 21, 2.2, 6, 2.3, 2.8, 4, 7 and 8 mJy at 319, 325, 333, 341, 355, 360, 375 and 380 MHz, respectively.

5. Discussion

5.1. Ordinary scintillation

We will first discuss the possibility that the event is the result of “ordinary” interstellar scattering. We assume a power law spectrum of density irregularities in the interstellar medium,

$$\Phi(\mathbf{k}) \propto k^{-\beta}, \quad (8)$$

where $k \equiv 2\pi/a$ is the wavevector associated with a particular spatial size a of the electron density inhomogeneities, and $\Phi(\mathbf{k})$ is the three-dimensional Fourier transform of the electron density correlation function $\langle N_e(\mathbf{x})N_e(\mathbf{x} + \mathbf{r}) \rangle$. For a Kolmogorov turbulence spectrum ($\beta = 11/3$), we have the following scaling laws for the decorrelation bandwidth, $\Delta\nu_d$, and the characteristic diffractive time scale, T_{dif} , of the scintillation,

$$\Delta\nu_d \propto \nu^{4.4} \quad (9)$$

$$T_{\text{dif}} \propto \nu^{1.2}. \quad (10)$$

(e.g., Lee & Jokipii 1975a, b, c; Rickett 1977; Manchester & Taylor 1977). A Kolmogorov spectrum over at least two orders of magnitude is consistent with observations (e.g., Armstrong et al. 1981).

Lyne (1984) observed for PSR B0655+64 a characteristic diffractive scintillation time scale of about 30 min. and a 50% decorrelation frequency of 1.1 MHz at 234 MHz. Using these values, we deduce a 50 % decorrelation bandwidth $\Delta\nu_d \approx 4.6$ MHz and a characteristic time scale $T_{\text{dif}} \approx 45$ min., for diffractive scintillation at 325 MHz. We observed a decorrelation bandwidth of $\Delta\nu_d = 3.6 \pm 0.4$ MHz and a characteristic time scale $\tau_d \approx 1$ hr. These results are in agreement with diffractive scintillation as the origin of the observed decorrelation bandwidth and the observed time scale of the variation in the flux density. However, the observed amplification of the flux density, a factor 69 ± 23 using Lorimer et al.’s (1995) long-term average flux density for PSR 0655+64, or a factor 43 ± 9 using our own long-term average 325 MHz flux density for PSR 0655+64, is very large.

The modulation index, m_I , of the intensity variations, $m_I \equiv \langle I^2 \rangle^{1/2} / \langle I \rangle$, consist of a diffractive, m_{dif} , and a refractive part, m_{ref} . Standard ISS theory (e.g., Lee & Jokipii 1975c) predicts a modulation index of DISS of about unity, $m_{\text{dif}} \sim 1$. Observations (e.g., Helfand et al. 1977) confirm this. Observations of RISS reveal that the refractive modulation index, m_{ref} is of the same order ($m_{\text{ref}} \sim 1$; e.g., Stinebring & Condon 1990). It is inconceivable that ordinary scintillation produces such a large amplification. This is particularly so, if one takes into account that the observing bandwidth $\Delta\nu$ of 5 MHz is not optimal for observing a phenomenon which exhibits a decorrelation bandwidth of $\Delta\nu_d \sim 3.6$ MHz. From Lee (1976) we find that, for a Kolmogorov spectrum, the modulation index m_{dif} is suppressed by about 25 per cent, by a rectangular band-pass, $\Delta\nu$ (for the above given values for $\Delta\nu$ and the observed $\Delta\nu_d$).

5.2. Caustics

We now discuss the possibility that the observed flux density amplification of PSR B0655+64 can be explained in terms of a caustic (strong focussing event).

In the following we use the model of Goodman et al. (1987). For a more detailed discussion we refer to this paper. We adopt the standard thin-screen approximation, i.e., the turbulent medium between the source and the observer is replaced by a single thin phase-changing screen. This is, of course, an approximation to scattering in an extended medium, but it might be well applicable to ‘enhanced’ scattering which is likely dominated by a localized clump of material, for example a super-nova remnant or an H II region.

Goodman et al. (1987) picture the scenario by a scattering screen, sub divided into a number of coherent patches from which radiation is received. The typical size of a coherent patch is $\sim r_{\text{dif}}$, where r_{dif} is the diffractive scale. Caustics can appear when the ISM turbulence is cut off at a scale r_c , the inner or cut-off scale, and when the inequality,

$$r_{\text{dif}} < r_c < r_{\text{ref}}, \quad (11)$$

holds; r_{ref} is the refractive scale. Now the cut-off scale r_c takes over as the typical size of a coherent patch. The caustics arise when neighbouring patches approach each other as a function of time and merge into a single (large and bright) patch. The caustic of lowest order is the fold caustic. The ratio $F_{\text{max,fold}}$ of the maximum flux over the mean flux for a fold caustic is

$$F_{\text{max,fold}} \sim \left(\frac{r_c}{r_{\text{ref}}} \right)^{7/3} \left(\frac{r_{\text{ref}}}{r_{\text{dif}}} \right)^{1/3}, \quad (12)$$

where we have used Eqs. 2.4.7, 3.2.8 and 3.3.6 from Goodman et al. (1987). Following Stinebring & Condon (1990) we can make an approximation for the RISS time scale T_{ref} , of PSR B0655+64 using

$$T_{\text{ref}} \approx \frac{4}{\pi} \left(\frac{\nu T_{\text{dif}}}{\Delta\nu_d} \right). \quad (13)$$

When the cut-off scale, r_c , is larger than the diffractive scale, r_{dif} , then the shape of the turbulence spectrum does not matter very much, the scattering behaves more like the Gaussian case, and the scaling laws are better approximated by $\Delta\nu_d \propto \nu^4$ and $T_{\text{dif}} \propto \nu$ (Narayan, private communications). Hence we find $\Delta\nu_d \sim 4.1$ MHz and $T_{\text{dif}} \sim 42$ min. (using Lyne’s values for T_{dif} and $\Delta\nu_d$). The expected RISS time scale for PSR B0655+64 is 2.9 days at 325 MHz. From this we find that $r_{\text{ref}}/r_{\text{dif}} \sim 100$ at 325 MHz, and hence

$$F_{\text{max,fold}} \sim 5 \left(\frac{r_c}{r_{\text{ref}}} \right)^{7/3}. \quad (14)$$

Since $r_c < r_{\text{ref}}$ the fold cannot explain the desired level of amplification. For the cusp caustic we have

$$F_{\text{max,cusp}} \sim \left(\frac{r_c}{r_{\text{ref}}} \right)^{5/2} \left(\frac{r_{\text{ref}}}{r_{\text{dif}}} \right)^{1/2} \sim 10 \left(\frac{r_c}{r_{\text{ref}}} \right)^{5/2}, \quad (15)$$

where we have used Eqs. 2.4.7, 3.2.8 and B8 from Goodman et al. (1987). The hyperbolic umbilic is the caustic of the next order. In one direction it is as a fold and in the other like a cusp caustic. We have

$$F_{\max, \text{hyp}} \sim \left(\frac{r_c}{r_{\text{ref}}}\right)^{17/6} \left(\frac{r_{\text{ref}}}{r_{\text{dif}}}\right)^{5/6} \sim 50 \left(\frac{r_c}{r_{\text{ref}}}\right)^{17/6}. \quad (16)$$

Eqs. 14, 15 and 16 give the order of magnitude of the types of caustics of the lowest order. To explain the event in terms of caustics, we have to interpret the flare as a diffractive modulation of a refractive envelope. The diffractive modulation can explain the duration of the flare (about one hr) and the narrow bandwidth of the phenomenon (3.6 ± 0.4 MHz; both in agreement with diffractive scintillation). The caustic itself can explain larger amplifications. Caustics are rare events (e.g., Goodman et al. 1987), and since the time scale of a caustic is smaller than the refractive time scale ($r_c < r_{\text{ref}}$), which is only 2.9 days for PSR B0655+64, this explains the lack of similar events at other days. However, in this context it is strange that the averages over the June 25 observation ($\bar{I}_{25\text{June}}$; Table 2), which give the best indication of the refractive “state” of the ISM on June 25, are so low; a diffractive modulation of a low level refractive envelope makes it hard to explain the huge amplification. Also we would expect to have observed several more diffractive scintels within the 6.3 hrs times 8 nearly independent bands (for diffractive scintillation) of June 25 (as is typical for dynamic spectra).

The next problem we encounter is that we need $r_c/r_{\text{ref}} \sim 1$ (Eqs. 14, 15 and 16), i.e., we need a small refractive scale r_{ref} , comparable to the cut-off scale r_c . Hence observations of systems with short refractive time scales are ideal, and PSR B0655+64 has a rather short expected refractive time scale. But, a statistical study of the relatively nearby ISM (< 1 kpc) by Armstrong et al. (1995) gives an upper-limit on the cut-off scale of $r_c \sim 10^8$ cm. The refractive scale of PSR B0655+64 is about 10^{12} cm (using the refractive time scale T_{ref} of 2.9 days and assuming a typical velocity v_{\perp} of 100 km/s). Hence still $r_c/r_{\text{ref}} \sim 10^{-4}$. So caustics as produced by a “normal” ISM seem inadequate to explain such a large amplification.

However, in search for a large cut-off scale, r_c , there is evidence that large scale structures of localized high density interstellar medium plasma exist, as for example has been postulated by Fiedler et al. (1987). Cordes et al. (1984) suggest a two-component model for the galactic electron density turbulence, consisting of a clumped medium with a scale height $H \leq 100$ pc and a nearly uniform medium for $H \geq 500$ pc. It is believed that ionization fronts associated with H II regions or shocks associated with stellar winds and supernova shells cause the so called Fiedler events (Fiedler et al. 1987). These events are also described in terms of caustics (e.g., Romani et al. 1987; Fiedler et al. 1994). However, Fiedler events have only been observed with much smaller amplification factors (< 5).

5.3. Intrinsic variation

An intrinsic event will be modulated by diffractive scintillation and hence explain the observed time scale (1 hr) and the ob-

served decorrelation bandwidth (3.6 ± 0.4 MHz). In order to explain the lack of similar increases at other times, and other frequencies within the 6.3 hrs of the June 25 observation, the duration of the event has to be of the order of the scintillation time scale (a few hours). However, there is overwhelming evidence that pulsars are intrinsically stable continuum sources on time scales of several minutes to weeks (e.g. Stinebring & Condon 1990; Kaspi & Stinebring 1992). We consider it quite unlikely that the event can be explained by intrinsic variability.

5.4. Other events

PSR B0655+64 was detected by Damashek et al. (1978) at a level of 40 mJy at 400 MHz. This is about 7-8 times higher than the long-term (average) flux density of the pulsar. The discovery therefore may have been made during another period of strong amplification, illustrating the (positive) effects of scintillation on the discovery of weak (nearby) pulsars. This, and our June 13 event, might indicate that at 92 cm extreme amplifications of a factor up to 8 for PSR B0655+64 are not extremely uncommon.

The increased probability of detection of a pulsar during periods of flux amplification may introduce a bias in the pulsar luminosity function, and affect the result of pulsar population studies. Johnston & Bailes (1991) note that pulsar surveys have been unable to significantly constrain the population of very low-luminosity millisecond pulsars. Correction for the bias requires a good understanding of the amplification factors.

6. Conclusions

A flux density amplification, which lasted about one hour, with a peak amplification of a factor 43 ± 9 has been observed for PSR B0655+64 at 325 MHz, June 25, 1994. The flare reached its maximum at MJD 49528.614. To the best of our knowledge such a large amplification has not been reported before. The phenomenon is restricted to a small bandwidth of 3.6 ± 0.4 MHz. The decorrelation bandwidth and characteristic time scale of the flux density amplification on June 25 at 325 MHz are in good agreement with the values expected for diffractive interstellar scintillation. However, the observed amplification of the flux density of PSR B0655+64 is rather large for this mechanism. The discovery observations of Damashek et al. (1978) and the amplification on June 13 suggest that amplifications of a factor up to 8 are not extremely uncommon for PSR 0655+64 at 92 cm. Possible explanations of the flux density amplification include caustics in the interstellar scintillation pattern. However, caustics produced by a “normal” ISM do not satisfactorily explain the huge amplitude of the amplification. We consider it quite unlikely that the event can be explained by intrinsic variability of the pulsar.

Acknowledgements. We thank Prof. Narayan for a fruitful discussion on caustics and Dr. Ramachandran for comments. We are grateful for the assistance of the WSRT telescope operators T. Spoelstra and R. de Haan. The WSRT is operated by the Netherlands Foundation for Research in Astronomy (NFRA) with financial aid by the Netherlands

Organization for Scientific Research (NWO). T. Galama is supported through a grant by NFRA under contract 781.76.011.

References

- Armstrong, J.W., Cordes, J.M., Rickett, B.J. 1981, Nat 291, 561
Blandford, R.D., Narayan, R. 1985, MNRAS 213, 591
Cognard, I., Shrauner, J.A., Taylor, J.H., Thorsett, S.E. 1996, ApJ, 457, L81
Coles, W.A., Frehlich, R.G., Rickett, B.J., Codona, J.L. 1987, ApJ 315, 666
Cole, T.W., Hesse, H.K., Page, C.G. 1970, Nat 225, 712
Cordes, J.M., Weisberg, J.M., Boriakoff, V. 1985 ApJ 288, 221
Damashek, M., Taylor, J.H., Hulse, R.A. 1978, ApJ 225, L31
Damashek, M., Backus, P.R., Taylor, J.H., Burkhardt, R.K. 1982, ApJ 253, L57
Fiedler, R.L., Dennison, B., Johnston, K.J., Hewish, A. 1987, Nat 326, 675
Fiedler, R.L., Dennison, B., Johnston, K.J., Waltman, E.B., Simon, R.S. 1994, ApJ 430, 581
Goodman, J.J., Narayan, R. 1985, MNRAS 214, 519
Goodman, J.J., Romani, R.W., Blandford, R.D., Narayan, R. 1987, MNRAS 229, 73
Helfand, D.J., Fowler, L.A., Kuhlman, J.V. 1977, AnJ 82, 701
Johnston, S., Bailes, M. 1991, MNRAS 252, 277
Jones, A.W., Lyne, A.G. 1988, MNRAS 232, 473
Kaspi, V.M., Stinebring, D.R. 1992, ApJ 392, 530
Kulkarni, S.R. 1986, ApJ 306, L85
Lee, L.C. 1976, ApJ 206, 744
Lee, L.C., Jorjipii, J.R. 1975a, ApJ 196, 695
Lee, L.C., Jorjipii, J.R. 1975b, ApJ 201, 532
Lee, L.C., Jorjipii, J.R. 1975c, ApJ 202, 439
Lorimer, D.R., Yates, J.A., Lyne, A.G., Gould, D.M. 1995, MNRAS 273, 411
Lyne, A.G. 1984, Nat 310, 300
Manchester, R.N., Taylor, J.H. 1977, *Pulsars*, Freeman, San Fransisco.
Narayan, R. 1992, Phil. Trans. R. Soc. Lond. A 341, 151
Rickett, B.J. 1977, ARAA 15, 479
Rickett, B.J. 1990, ARAA 28, 561
Rickett, B.J., Lyne, A.G. 1990, MNRAS 244, 68
Rickett, B.J., Coles, W.A., Bourgois, G. 1984, A&A 134, 390
Romani, R.W., Blandford, R.D., Cordes, J.M. 1987, Nat 328, 324
Salpeter, E.E. 1969, Nat 221, 31
Scheuer, P.A.G. 1968, Nat 218, 920
Stinebring, D.R., Condon, J.J. 1990, ApJ, 352, 207
Taylor, J.H., Manchester, R.N., Lyne, A.G. 1993, ApJ 88, 529
Van den Oord, G.H.J., De Bruyn, A.G. 1994, A&A 286, 181
Wieringa, M.H. 1992, Exp. Astr. 2, 203